HHS Public Access

Author manuscript

Neurosurgery. Author manuscript; available in PMC 2016 May 04.

Published in final edited form as:

Neurosurgery. 2014 November ; 75(5): 515–522. doi:10.1227/NEU.0000000000000507.

MRI Measures of Posterior Cranial Fossa Morphology and CSF Physiology in Chiari Malformation Type I

Noam Alperin, PhD[1], **James Ryan Loftus, BS**[1], **Carlos J. Oliu, BS**[1], **Ahmet Bagci, PhD**[1], **Sang H. Lee, MS**[1], **Birgit Ertl-Wagner, MD**[3], **Barth Green, MD**[2], and **Raymond Sekula, MD**[4]

[1]Department of Radiology, University of Miami, Miami, FL

[2]Department of Neurological Surgery, University of Miami, Miami, FL

[3]Department of Radiology, University of Munich, Munich, Germany

[4]Neurological Surgery, University of Pittsburgh, PA, USA

Abstract

Background—It has been well documented that along with tonsillar herniation, Chiari Malformation Type I (CMI) is associated with smaller posterior cranial fossa (PCF) and altered CSF flow and tissue motion in the cranio-cervical junction (CCJ).

Objective—This study assesses the relationship between PCF volumetry and CSF and tissue dynamics toward a combined imaging-based morphologic-physiologic characterization of CMI. Multivariate analysis is employed to identify the subset of parameters that best discriminates CMI from healthy.

Methods—Eleven length and volumetric measures of PCF, including volume, crowdedness, and 4th ventricle volume, four measures of CSF and cord motion in the CCJ, and five global intracranial measures, including intracranial compliance and pressure, were measured by MRI in 36 symptomatic CMI subjects (28F, 37±11 years) and 37 control subjects (24F, 36±12 years). The CMI group was further divided based on symptomatology into “typical” and “atypical” subgroups.

Results—Ten of the 20 morphologic and physiologic measures were significantly different between the CMI and the control cohorts. These parameters also had less variability and stronger significance in the typical CMI compared with the atypical. The measures with the most significance were clival and supraocciput lengths, PCF crowdedness, normalized PCF volume, 4th ventricle volume, maximal cord displacement ($p<.001$), and MR measure of ICP ($p=.007$). Multivariate testing identified cord displacement, PCF crowdedness, and normalized PCF as the strongest discriminator subset between CMI and controls. MRICP was higher in the typical CMI cohort compared with the atypical.

Corresponding author: Noam Alperin, Department of Radiology, University of Miami, Professional Arts Center, Suite 713, 1150 N.W. 14th Street, Miami, FL 33136, Phone: 305-243-8098, Fax: 305-243-3405, Nalpeirn@med.miami.edu.

Disclosure: The authors have no personal, financial, or institutional interest in any of the drugs, materials, or devices described in this article. Supported by NIH grant no 7R01NS052122.

Conclusion—The identified 10 complementing morphologic and physiologic measures provide a more complete and symptomatology relevant characterization of CMI than tonsillar herniation alone.

Keywords

Chiari Malformation; Posterior Cranial Fossa Morphology; CSF flow Dynamics; MRI; Quantitative measures

INTRODUCTION

Chiari Malformation Type I (CMI) is a complex neurosurgical problem classically defined as cerebellar tonsil herniation ≥ 5mm below the foramen magnum.[1] Commonly associated symptomatology includes suboccipital headaches (aggravated by Valsalva) and sensory and motor deficits. Suboccipital decompressive surgery is a standard treatment for CMI, but outcome is poor in approximately 3 in 10 patients.[2] The degree of tonsillar herniation has not been a reliable predictor of either symptom severity[3] or surgical outcome.[4] Along with tonsillar herniation, imaging studies have documented additional abnormalities, including smaller and overcrowded posterior cranial fossa (PCF),[5–9] altered CSF flow in the craniocervical junction,[10–13] hyperdynamic tonsils and cord motion,[14–16] and lower intracranial compliance.[17]

The size of the PCF is often approximated using linear markers measured in CT scans and mid-sagittal T1-weighted MR sequences.[5–7] The lengths of the clivus, supraocciput, and exocciput were generally found to be shorter in CMI compared to a healthy cohort.[5–7] However, significance levels and thresholds varied amongst studies.[5–7] Laborious manual measurement of the PCF volume via the Cavalieri method on CT images demonstrated significantly reduced PCF volume in CMI compared to controls.[6, 8] Limited evidence suggests that PCF volumetry, though not associated with the degree of herniation, is a potential predictor of surgical outcome.[9] A preliminary comparison between PCF volumetry and linear markers revealed that none of the mid-sagittal length measures are strong standalone predictors of the PCF volume.[18]

Other groups focused on CSF flow and tissue movement dynamics in the craniocervical junction (CCJ) using velocity encoded MR imaging. Studies of CMI reported both decreased[10, 11] and increased[12] CSF velocity in different regions of interest, and greater CSF velocity fluctuations.[13] Better consensus was reported on the hyperdynamic tonsillar and cord tissue movement during the cardiac cycle.[14–17] Caudal velocities of the tonsils[14] and tonsillar pulsations[15] were increased in CMI patients, along with increased systolic and diastolic cord displacement rates,[16] and maximal cord displacement at the C2 level.[17] In addition to local changes at the CCJ, global hydrodynamic changes such as reduced MRI measure of intracranial compliance (ICC) were also reported.[17]

This study employs various MRI techniques to quantify morphologic measures, tissue and CSF motion dynamics, and global craniospinal hydrodynamics in the same CMI cohort, in order to study the interplay between these factors, and then identifies a subset of these

parameters that best differentiates CMI from non-CMI patients. The study also explores whether linear PCF markers are reliable estimates of the PCF volume.

METHODS

Subjects

Following IRB approval and written informed consent, 36 newly diagnosed symptomatic CMI patients (28 females; 37±11 years) with tonsillar herniation >5mm were enrolled at a single center. The CMI cohort was divided into two subgroups, patients with symptoms typical to CMI (typical CMI), and with symptoms that are less common in CMI (atypical CMI). Typical CMI symptoms include Valsalva-induced suboccipital headache and upper/lower extremity numbness. The most common atypical symptoms included: non-suboccipital, non-Valsalva induced headache, neck pain, vision problems, hearing/equilibrium problems (vertigo, tinnitus, poor coordination, gait problems, dizziness/blackouts), facial pain/numbness, and muscle weakness. The less common atypical symptoms included dysphagia, sleep apnea and tremors. Of the 36 patients, 19 were classified as typical (age 36±11 years) and 17 as atypical CMI (age 37±10). During the study period, five of the typical and four of the atypical CMI patients underwent minimal sub-occipital decompression surgery. All surgical patients except for two of the atypical CMI had a favorable outcome. Additionally, 37 healthy subjects (24 females; 36±12 years) without history of neurological problems were recruited as a control cohort.

MRI acquisition and Data analysis

MR imaging was performed using 1.5T (Excite, GE Healthcare, Milwaukee, WI) and 3T (Magnetom Verio, Siemens Healthcare, Erlangen, Germany) scanners. The imaging protocol included a 3-D T1-W scan for the morphological assessment and two cine velocity encoded phase contrast scans, one with high velocity encoding (70–80cm/s) for imaging the arterial and venous blood flows to and from the cranium, and the second with low velocity encoding (7–8cm/s) for imaging the CSF flow and cord motion at the upper cervical region. Voxel sizes for the 3-D T1-W sequence were similar on both scanners using MPRAGE technique on the Siemens scanner and SPGR on the GE scanner. Pixel size was 0.9×0.9mm, with a slice thickness of 1~1.5 mm. The voxel dimensions for the phase contrast scans were also similar; using a pixel size of approximately 0.56×0.6mm and slice thickness of 5–6mm. The MRI derived anatomical and physiological parameters were divided into the following classes: linear and 3-D PCF morphology, flow and motion dynamics in the CCJ, and global intracranial measures as listed in Table 1.

Linear PCF Measures

The lengths of the clivus (inferior boundary of the dorsum sellae to the basion), supraocciput (opisthion to the internal occipital protuberance), McRae's line (basion to the opisthion), and Twining's line (inferior boundary of the dorsum sellae to the internal occipital protuberance) were manually measured on the mid-sagittal slice of the 3-D T1-weighted MR image using in-house DICOM image display utility by a single experienced observer (SHL with 10 years experience). PCF length measures were included for comparison with previous reports and for testing associations with the volumetric PCF measures.

Volumetric PCF Measures

A previously validated automated atlas-based method for PCF volumetry[18] was applied to quantify the PCF volume (PCFV), the hindbrain volume, and the volume of the 4th ventricle. That method utilizes a tailored brain atlas created using images from CMI patients to guide the segmentation of the PCF.[18] The 4th ventricle, lateral ventricles, and hindbrain volumes were segmented using Freesurfer.[19] An example of the linear measures and a rendering of the PCF volume are shown in Figure 1.

CSF Flow and Cord Motion Measures

The methods for automated quantitation of the blood and CSF volumetric flow rates and the derivation of intracranial compliance and pressure by MRI have been previously described.[20–22] Briefly, mean velocities and volumetric flow rates through vessels and the upper cervical CSF lumen are obtained for each of the 32 velocity encoded images composing a complete cardiac cycle. The blood vessels and CSF lumens are segmented using the Pulsatility Based Segmentation (PUBS) method, which utilizes the dynamic information throughout the cardiac cycle and a cross correlation method to differentiate lumen from the background pixels and delineate the lumen boundary.[22] Mean flow rate is then calculated by integrating all the pixels within the delineated lumen. Mean velocity is the average velocity within the lumen boundary. Upper cervical CSF stroke volume (SV) is derived by time integration of the absolute values of the CSF volumetric flow rate waveform and division by two after subtraction of the net flow. It represents the CSF volume that moves back and forth between the cranium and spinal canal during one cardiac cycle. Maximal cord displacement during the cardiac cycle is obtained by time integration of the average velocity waveform obtained in a region of interest inside the cord.

Global Intracranial Parameters

The method for derivation of intracranial compliance and pressure by MRI (MRICP) has been previously described in detail[20] and was recently independently validated.[23] Briefly, intracranial compliance (ICC) is inversely related to intracranial pressure (ICP) because of the mono-exponential relationship between pressure and volume. ICC is derived from the ratio of intracranial volume and pressure changes during the cardiac cycle. The change in intracranial volume during the cardiac cycle (ICVC) is derived from the momentary differences between the total cerebral blood inflow (tCBF), venous blood outflow, and cranio-spinal CSF that enter and leave the cranium during the cardiac cycle. The maximal change in pressure due to the maximal change in volume during the cardiac cycle is derived from the change in the CSF pressure gradient, which is calculated using the Navier-Stokes relationship between pressure gradients and temporal and spatial derivatives of the cranio-spinal CSF velocities.[20, 24] The total cerebral blood inflow is derived by summation of the flow through the internal carotid and vertebral arteries. The venous outflow is derived by summation of the flow through the internal jugular veins and secondary venous channels (e.g., epidural and vertebral veins) when present.

Statistical Analysis

A paired, 2-tailed t-test was applied to determine the significance of measurements between the healthy and CMI cohorts, as well as between the healthy and the individual typical and atypical CMI sub-cohorts. Dependency and association between linear and 3-D measures of PCF morphology and between the morphological and physiological measures were investigated using linear regression. Finally, a series of multivariate analyses was employed to determine the combination of morphologic and physiologic parameters that best differentiates the CMI subjects from healthy controls. Initially, a binary logistic regression was applied to each parameter individually to determine its significance in classifying group membership. Significance of $p < .2$ was used as a criterion for parameter inclusion to prevent the elimination of variables that may be significant in the second step, backward likelihood logistic regression analysis. Elimination of the parameters continues until the goodness-of-fit of the logistic model as well as the probability of correctly classifying normal and CMI cases is maximized. Finally, a discriminant analysis was performed to quantify the overall percentage of cases correctly classified based on the variables remaining from the previous logistic regression analyses. Analyses were performed using SPSS version 20 (SPSS, Chicago, IL).

RESULTS

Ten of the 20 tested morphologic and physiologic measures were significantly different between the CMI and the control cohorts. Furthermore, significance levels were mostly stronger in the typical CMI sub-cohort compared to the atypical CMI sub-cohort. The mean and SD values of the 20 measures and their significance levels are listed in order of relative significance in Table 2. The PCF morphology measures that demonstrated the strongest significance when comparing CMI patients to the control cohort were: clival and supraocciput lengths in the linear measures category, and PCF crowdedness (Hindbrain/PCFV), PCF volume (PCFV), PCF volume normalized for intracranial volume (PCFV/ICV), and the 4^{th} ventricle volume in the 3-D category. In contrast to the 4^{th} ventricle and PCF volumes, neither the lateral ventricles nor the intracranial volume (ICV) were different. Out of the four cervical CSF flow and cord motion measures, only the maximal cord displacement was significantly different between the CMI and the healthy cohorts. An example of cord motion and displacement waveforms from a representative control and from a CMI patient is shown in Figure 2. The mean maximal cord displacement was more than twice as large in the CMI cohort compared to the control cohort, with a mean and SD values of 0.373±0.198 and 0.174±0.047mm, respectively. In contrast, the cervical CSF stroke volume was similar in both cohorts (0.54±0.17 and 0.54±0.18mL, respectively). Finally, among the global intracranial hydrodynamics measures, the MR derived intracranial compliance values were significantly lower and consequently, the MRICP values significantly higher, in the typical CMI sub-cohort relative to the atypical CMI sub-cohort and the control cohort.

Association within and between the 1-D and 3-D PCF morphological measures

The clivus and supraocciput lengths were neither correlated in the CMI cohort nor correlated in the healthy cohort. The scatter plots and the linear regression lines between the clivus and

supraocciput lengths for the CMI cohort and the healthy cohort are shown in Figure 3. The R values between the clivus and supraocciput lengths, as well as between these linear measures and the 3-D measures (PCFV and 4th ventricles) are listed in Table 3. In general, the testing for dependency between the linear and 3-D PCF measures demonstrated mostly a weak correlation, with only a few measures reaching moderate range correlation of around .4. The supraocciput length was the only linear measure that was significantly correlated with 3-D measures in the CMI cohort, i.e., the PCFV (R=.40), and the 4th ventricle volume (R=.37). None of the linear PCF measures was significantly correlated with the 3-D measures in the healthy cohort.

Association between morphological and CSF Flow and Cord Motion Measures

Similar to the relationships between the linear and volumetric PCF measures, mostly weak and non-significant correlations were found between the PCF and the CSF and cord motion at the CCJ within either cohort. The only correlation that reached significance was between the peak systolic mean CSF velocity and the PCFV in the healthy cohort, with R=.33 (P=.04). When pooling the CMI and healthy cohorts together, parameters with large differences between CMI and controls reach significant correlation because of the wider latitude of the parameters and the larger N. Pearson correlations and P values for the tested linear regression between the PCF measures and CSF flow and cord motion measures are listed in Table 3.

Association with intracranial measures

Out of the five global intracranial measures, three demonstrated mild significant correlations within the CMI cohort. The maximal volume change during the cardiac cycle (ICVC) was correlated with the PCFV (R=.33, P=.04) and with the 4th ventricle volume (R=.39, P=.01). The intracranial compliance index (ICCI) was mildly correlated with the 4th ventricle volume (R=.47, P=.004), and finally, MRICP was mildly correlated with PCF crowdedness, 4th ventricle volume, PCFV, and normalized PCFV in the combined cohort only. The R and P values for the intracranial measures are listed in Table 3.

Multivariate analyses

The multivariate analyses identified a subset of three out of the 20 measures that best differentiate CMI from the healthy cohort: maximal cord displacement, normalized PCFV (PCFV/ICV), and PCF crowdedness. With these three parameters, 37 of the 37 healthy subjects were correctly classified as non-CMI and 35 of the 36 CMI were correctly classified as CMI (sensitivity of 97.3% and specificity of 100%). The “misclassified” CMI patient belonged to the atypical cohort. Of the four atypical CMI patients who underwent decompression, the two who did not improve following surgery were found to have several measures not within the CMI range: clivus and maximal cord displacement in the first patient, and supraocciput and MRICP in the second patient.

DISCUSSION

Previous imaging-based investigations exploring features characteristics of CMI focused on a specific class of features (e.g., linear PCF markers, CSF velocities in the upper cervical

regions) in different CMI patient cohorts to identify potential markers of CMI. This study expands upon these studies by comparing a wide range of morphologic and physiologic measures in the same CMI patients and matched control subjects, thereby providing means to determine the relative significance of each parameter, with respect to the others, as markers of CMI. The study indentifies 10 morphologic and physiologic measures that were significantly different between the patient and control cohorts and therefore can be used as markers of CMI. Out of these 10 parameters, a subset of 2 linear PCF measures, 4 volumetric PCF measures, and one physiologic measure demonstrated the strongest discrimination power. The other parameters that were less significant did contribute to the identification of the only two patients who did not improve following decompression surgery.

Smaller length and volumetric PCF measures observed in our CMI cohort are in agreement with previous observations.[5–9] The most significant linear measures were the clivus and supraocciput lengths, and the most significant volumetric measures were the absolute and normalized PCF volumes, the PCF crowdedness, and the 4th ventricle volume. Normalized PCFV and PCF crowdedness were much more significant than the non-normalized PCF volume, indicating that CMI is better characterized by the volume of the PCF in relation to the intracranial volume of the cranium and the crowdedness of the PCF. A smaller than normal 4th ventricle with normal size lateral ventricles has not been previously described in CMI. This is consistent with PCF overcrowding. Along with these findings, our study also reaffirms previously reported significantly larger cord displacement and lower intracranial compliance in CMI.[16, 17]

The current study reveals differences in certain morphologic and physiologic parameters between symptom types (typical vs. atypical CMI), primarily PCF crowdedness, 4th ventricle volume and MRICP, which are considerably less variable in the typical subgroup compared with the atypical. The intracranial compliance and MRICP were significantly different from controls only in the typical CMI subgroup. This is consistent with previously reported findings of lower ICC in another typical CMI cohort whose main symptoms included suboccipital headaches.[17] The systolic (peak) CSF velocities demonstrated no difference between CMI (either typical or atypical) and the control cohort. This finding is in agreement with Krueger et al.'s work showing no difference in peak CSF velocities between symptomatic and asymptomatic CMI patients. [25] These results do not support the commonly held view that CMI involves "blockage" of CSF flow in the CCJ and the subjective assessments that CSF flow in the CCJ is more "abnormal" in symptomatic CMI compared with asymptomatic tonsillar ectopia patients.[26]

The study further suggests that the commonly used PCF length measurements provide only a coarse estimate of the PCF volume. Testing the degree of association between the linear and the volumetric measures revealed that these measures were not correlated within each cohort, except for the supraocciput length, which was mildly associated with the PCF and the 4th ventricle volumes in the CMI cohort. These findings indicate that the linear measures are complementing the volumetric measures.

In summary, this is the first study that quantifies both the morphologic and physiologic measures in the same CMI cohort. The study reveals either weak or no associations between these measures, thereby demonstrating the independency and the complementary nature of these parameters.

One of the aims of the study was to identify a concise multi-parametric characterization of CMI that is better associated with the complex symptomatology than the degree of tonsillar herniation. A multivariate binary logistic regression employed to obtain a data driven model identified 3 parameters out of the 20 measures as the strongest characterization of CMI: normalized PCFV (PCFV/ICV), PCF crowdedness, and maximal cord displacement. Using only these 3 parameters, all 37 healthy subjects were correctly classified as non-CMI and 35 of the 36 CMI subjects were correctly classified as CMI. The “misclassified” patient was from the atypical subgroup (e.g., right side papilledema). This patient’s normalized PCFV was normal due to a smaller than normal intracranial volume. In follow-up consultations her neurologist and neurosurgeon revised her diagnosis, as it was felt that her symptoms were unrelated to her CMI regardless of a tonsillar herniation of 7mm.

Limitations

This study has several limitations that need to be taken into account when interpreting the data. The identified discriminators between CMI and controls are specific to the cohorts used in this study, and additional studies of other CMI and control cohorts are needed to confirm these findings. Second, asymptomatic CMI subjects were not included in this study and, therefore, imaging-based features specific to the onset of symptoms could not be investigated. Third, the long-term goal of determining the predictive values of the CMI markers for surgical outcome requires a large number of patients that undergo surgical treatment during the study. In the current study period, only nine patients underwent surgical treatment and only two of them had poor outcome. Therefore, while the available data is sufficient for identifying the CMI discriminators, it is insufficient for establishing their predictive value for surgical outcome. In the only two patients (both atypical CMI) in whom symptoms persisted post-surgery, several primary CMI markers were outside the CMI range, i.e., cord displacement and clivus length in the first patient and supraocciput length and MRICP in the second patient. These results warrant investigations with larger number of post-surgical patients to assess the efficacy of the identified morphologic and physiologic measures as predictors of surgical outcome.

CONCLUSION

This study identified 10 imaging-based morphologic and physiologic quantitative parameters that are associated with CMI symptomatology and thus may be more clinically relevant characteristics of CMI than the degree of tonsillar herniation alone.

References

1. Elster AD, Chen MY. Chiari I malformations: clinical and radiologic reappraisal. Radiology. May; 1992 183(2):347–353. [PubMed: 1561334]

2. Aliaga L, Hekman KE, Yassari R, et al. A novel scoring system for assessing Chiari malformation type I treatment outcomes. Neurosurgery. Mar; 2012 70(3):656–664. discussion 664–655. [PubMed: 21849925]

3. Khan AA, Bhatti SN, Khan G, et al. Clinical and radiological findings in Arnold Chiari malformation. Journal of Ayub Medical College, Abbottabad : JAMC. Apr-Jun;2010 22(2):75–78. [PubMed: 21702272]

4. Noudel R, Gomis P, Sotoares G, et al. Posterior fossa volume increase after surgery for Chiari malformation Type I: a quantitative assessment using magnetic resonance imaging and correlations with the treatment response. Journal of neurosurgery. Sep; 2011 115(3):647–658. [PubMed: 21294619]

5. Nishikawa M, Sakamoto H, Hakuba A, Nakanishi N, Inoue Y. Pathogenesis of Chiari malformation: a morphometric study of the posterior cranial fossa. Journal of neurosurgery. Jan; 1997 86(1):40–47. [PubMed: 8988080]

6. Milhorat TH, Chou MW, Trinidad EM, et al. Chiari I malformation redefined: clinical and radiographic findings for 364 symptomatic patients. Neurosurgery. May; 1999 44(5):1005–1017. [PubMed: 10232534]

7. Karagoz F, Izgi N, Kapijcijoglu Sencer S. Morphometric measurements of the cranium in patients with Chiari type I malformation and comparison with the normal population. Acta neurochirurgica. Feb; 2002 144(2):165–171. discussion 171. [PubMed: 11862517]

8. Milhorat TH, Nishikawa M, Kula RW, Dlugacz YD. Mechanisms of cerebellar tonsil herniation in patients with Chiari malformations as guide to clinical management. Acta neurochirurgica. Jul; 2010 152(7):1117–1127. [PubMed: 20440631]

9. Badie B, Mendoza D, Batzdorf U. Posterior fossa volume and response to suboccipital decompression in patients with Chiari I malformation. Neurosurgery. Aug; 1995 37(2):214–218. [PubMed: 7477771]

10. Armonda RA, Citrin CM, Foley KT, Ellenbogen RG. Quantitative cine-mode magnetic resonance imaging of Chiari I malformations: an analysis of cerebrospinal fluid dynamics. Neurosurgery. Aug; 1994 35(2):214–223. discussion 223–214. [PubMed: 7969828]

11. Bhadelia RA, Bogdan AR, Wolpert SM, Lev S, Appignani BA, Heilman CB. Cerebrospinal fluid flow waveforms: analysis in patients with Chiari I malformation by means of gated phase-contrast MR imaging velocity measurements. Radiology. Jul; 1995 196(1):195–202. [PubMed: 7784567]

12. Haughton VM, Korosec FR, Medow JE, Dolar MT, Iskandar BJ. Peak systolic and diastolic CSF velocity in the foramen magnum in adult patients with Chiari I malformations and in normal control participants. AJNR. American journal of neuroradiology. Feb; 2003 24(2):169–176. [PubMed: 12591629]

13. Quigley MF, Iskandar B, Quigley ME, Nicosia M, Haughton V. Cerebrospinal fluid flow in foramen magnum: temporal and spatial patterns at MR imaging in volunteers and in patients with Chiari I malformation. Radiology. Jul; 2004 232(1):229–236. [PubMed: 15155896]

14. Wolpert SM, Bhadelia RA, Bogdan AR, Cohen AR. Chiari I malformations: assessment with phase-contrast velocity MR. AJNR. American journal of neuroradiology. Aug; 1994 15(7):1299–1308. [PubMed: 7976942]

15. Pujol J, Roig C, Capdevila A, et al. Motion of the cerebellar tonsils in Chiari type I malformation studied by cine phase-contrast MRI. Neurology. Sep; 1995 45(9):1746–1753. [PubMed: 7675239]

16. Hofmann E, Warmuth-Metz M, Bendszus M, Solymosi L. Phase-contrast MR imaging of the cervical CSF and spinal cord: volumetric motion analysis in patients with Chiari I malformation. AJNR. American journal of neuroradiology. Jan; 2000 21(1):151–158. [PubMed: 10669242]

17. Alperin N, Sivaramakrishnan A, Lichtor T. Magnetic resonance imaging-based measurements of cerebrospinal fluid and blood flow as indicators of intracranial compliance in patients with Chiari malformation. Journal of neurosurgery. Jul; 2005 103(1):46–52. [PubMed: 16121972]

18. Bagci AM, Lee SH, Nagornaya N, Green BA, Alperin N. Automated Posterior Cranial Fossa Volumetry by MRI: Applications to Chiari Malformation Type I. AJNR. American journal of neuroradiology. 2013; 34(9):1758–63. [PubMed: 23493894]

19. Fischl B, Salat DH, Busa E, et al. Whole brain segmentation: automated labeling of neuroanatomical structures in the human brain. Neuron. Jan 31; 2002 33(3):341–355. [PubMed: 11832223]
20. Alperin NJ, Lee SH, Loth F, Raksin PB, Lichtor T. MR-Intracranial pressure (ICP): a method to measure intracranial elastance and pressure noninvasively by means of MR imaging: baboon and human study. Radiology. Dec; 2000 217(3):877–885. [PubMed: 11110957]
21. Alperin N, Mazda M, Lichtor T, Lee SH. From Cerebrospinal Fluid Pulsation to Noninvasive Intracranial Compliance and Pressure Measured by MRI Flow Studies. Current Medical Imaging Reviews. 2006; 2:117–129.
22. Alperin N, Lee SH. PUBS: pulsatility-based segmentation of lumens conducting non-steady flow. Magnetic resonance in medicine : official journal of the Society of Magnetic Resonance in Medicine / Society of Magnetic Resonance in Medicine. May; 2003 49(5):934–944.
23. Muehlmann M, Koerte IK, Laubender RP, et al. Magnetic resonance-based estimation of intracranial pressure correlates with ventriculoperitoneal shunt valve opening pressure setting in children with hydrocephalus. Investigative radiology. Jul; 2013 48(7):543–547. [PubMed: 23695081]
24. Loth F, Yardimci MA, Alperin N. Hydrodynamic modeling of cerebrospinal fluid motion within the spinal cavity. Journal of biomechanical engineering. Feb; 2001 123(1):71–79. [PubMed: 11277305]
25. Krueger KD, Haughton VM, Hetzel S. Peak CSF velocities in patients with symptomatic and asymptomatic Chiari I malformation. AJNR. American journal of neuroradiology. Nov; 2010 31(10):1837–1841. [PubMed: 20884747]
26. Hofkes SK, Iskandar BJ, Turski PA, Gentry LR, McCue JB, Haughton VM. Differentiation between symptomatic Chiari I malformation and asymptomatic tonsilar ectopia by using cerebrospinal fluid flow imaging: initial estimate of imaging accuracy. Radiology. Nov; 2007 245(2):532–540. [PubMed: 17890352]

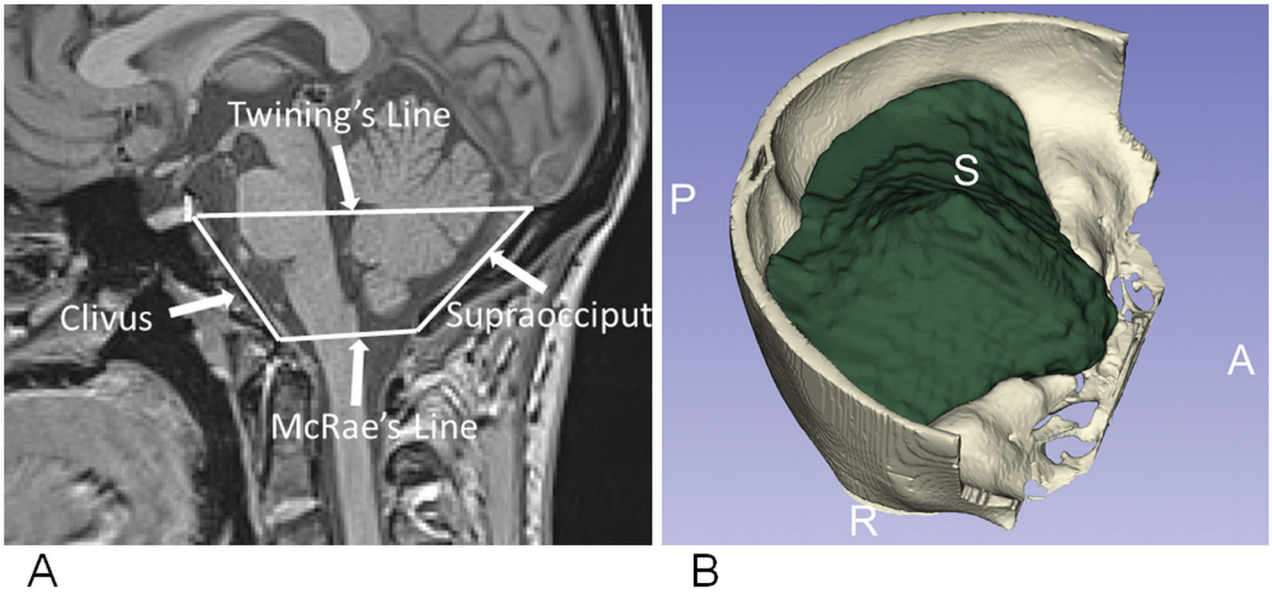

Figure 1.

A) The linear measures of the PCF: Clivus, supraocciput, McRae's line, and Twining's line, superimposed on mid-sagittal slices of 3-D T1-weighted MR images. B) A rendering of the automated PCF volume segmentation.

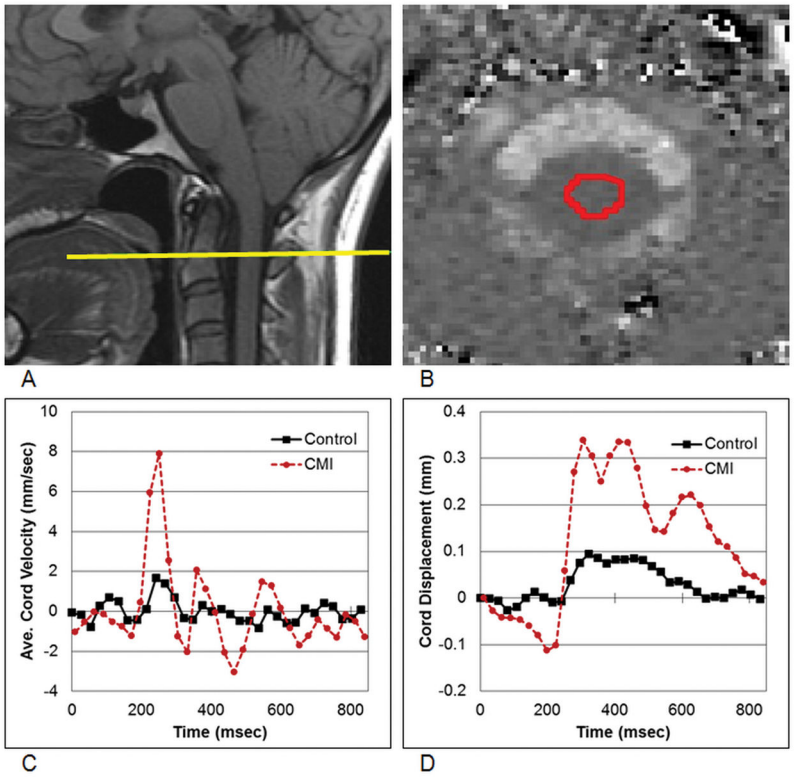

Figure 2.

Measurements of cord motion dynamics. A) The imaging plane superimposed on the MRI mid-sagittal image in a CMI patient. (B) The cord region of interest superimposed on the MRI phase contrast velocity image. C) Average cord velocity waveforms for a representative CMI and control patient. D) Cord displacement waveforms from the representative CMI and control patient obtained by integration of the velocity waveforms with respect to time for one cardiac cycle.

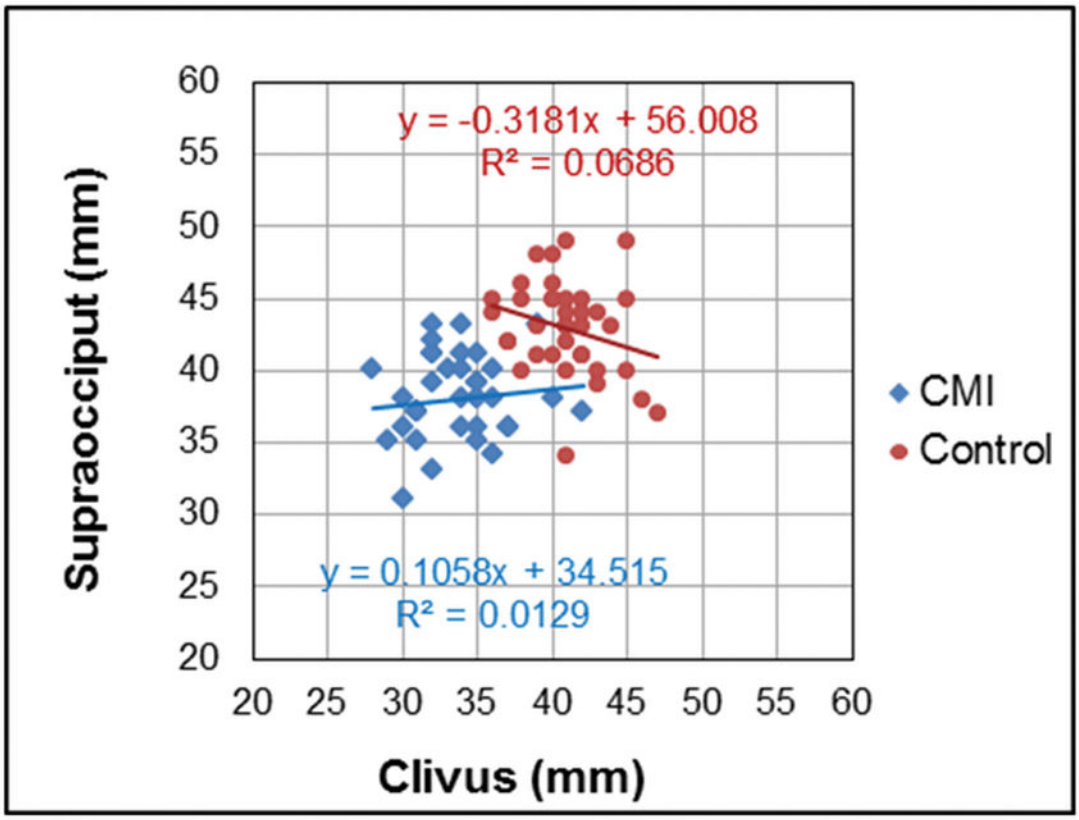

Figure 3.
Association between clivus and supraocciput length measurements. Linear regressions for the CMI (diamonds) and control (circles) cohorts do not show statistical significance.

Table 1

Quantitative morphologic and dynamic measures derived from the MRI scans

Linear PCF Measures	Volumetric PCF Measures	CSF Flow and Cord Movement in the CCJ	Intracranial Measures
Clivus	Intracranial Volume (ICV)	CSF Stroke Volume (SV)	Total Cerebral Blood Flow (TCBF)
Supraocciput	PCF Volume (PCFV)	Systole CSF Velocity	Intracranial Volume Change (ICVC)
Twining's Line	Hindbrain Volume	Diastole CSF Velocity	Pulse Pressure Gradient (PTP-PG)
McRae's Line	4th Ventricle Lateral Ventricles	Max. Cord Displacement	Intracranial Compliance index (ICCI) Intracranial Pressure (MR-ICP)

Table 2

Mean and standard deviation of quantitative morphologic and dynamic measures in the order of significance (t-Test) between control and CMI (typical + atypical) groups

	Control	CMI	Typical CMI	Atypical CMI
1D Morphology				
Clivus (mm)	41.0±2.7	33.7±3.1**	33.5±2.9**	34.0±3.4**
Supraocciput (mm)	43.0±3.3	38.1±2.9**	38.1±3.0**	38.1±2.7**
Twining's Line (mm)	82.9±3.7	80.9±4.2*	80.9±3.6	80.9±4.9
McRae's Line (mm)	36.8±2.4	37.6±3.5	37.8±3.3	37.3±3.9
Tonsil. Herniation (mm)		9.1±3.5	9.5±3.3†	8.5±3.7†
3D Morphology (Volumes)				
Hindbrain/PCFV	0.793±0.036	0.880±0.038**	0.876±0.026**	0.883±0.049**
PCFV/ICV	0.140±0.008	0.124±0.008**	0.123±0.009**	0.125±0.008**
PCFV (mL)	211±16	184±19**	184±19**	184±19**
4th Ventricle Volume (mL)	2.19±0.69	1.43±0.48**	1.35±0.38**	1.52±0.57**
Hindbrain Volume (mL)	167±16	162±16	161±16	163±17
Lateral Ventricle Volume (mL)	16.1±7.2	15.2±7.5	14.9±8.5	15.5±6.4
ICV (mL)	1505±109	1489±156	1495±142	1482±174
CSF Flow Measurements				
Cord Displacement (μm)	174±47	373±198**	359±118**	387±264*
CSF Systole Velocity (mm/s)	17.4±5.7	16.1±5.0	17.4±5.1	14.6±4.5
CSF Diastole Velocity (mm/s)	9.4±3.0	9.7±3.8	10.1±4.3	9.2±3.3
CSF Stroke Volume (mL)	0.54±0.18	0.54±0.17	0.55±0.19	0.52±0.15
Intracranial Parameters				
MR-ICP (mmHg)	8.8±2.3	12.7±6.3*	13.6±5.9*	11.8±6.7
ICC Index	8.7±3.1	6.8±3.3*	6.1±2.9*	7.6±3.5
ICVC (mL)	0.52±0.16	0.45±0.20	0.44±0.21	0.45±0.21
PTP-PG (mmHg/cm)	0.035±0.011	0.036±0.011	0.039±0.011	0.035±0.011
TCBF (mL/min)	776±107	764±99	765±95	762±106

*P<.05

**p<.001

†Tonsillar herniation of typical and atypical CMI are not significantly different (p-value=.4)

Table 3

Summary of associations levels between CMI parameters

	CMI only		Control only		CMI + Control	
Linear vs. Linear	**R**	**p-value**	**R**	**p-value**	**R**	**p-value**
Clivus vs. Supraocciput	.114	.51	−.262	.11	.457	**.001**
Linear vs. 3D						
Clivus vs. 4th Vent	.026	.87	.213	.21	.509	**.001**
Clivus vs. PCFV	.127	.46	.316	.05	.587	**.001**
Supraocciput vs. 4th Vent.	.369	**.02**	−.039	.82	.454	**<.001**
Supraocciput vs. PCFV	.404	**.01**	.281	.09	.596	**<.001**
CSF/Cord motion vs. 3D						
CSF Sys. Vel. vs. PCFV	−.036	.82	.334	**.04**	.190	0.10
Cord Disp. vs. HBV/PCFV	.139	.42	.087	.61	.498	**<.001**
Cord Disp. vs. PCFV/ICV	−.111	.52	.069	.66	−.446	**<.001**
Cord Disp. vs. PCFV	−.025	.88	−.057	.73	−.373	**.001**
Intracranial Param. Vs. 3D						
MRICP vs. HBV/PCFV	.009	.96	.096	.57	.315	**.007**
MRICP vs. PCFV/ICV	−.028	.87	−.342	.84	−.296	**.01**
MRICP vs. PCFV	−.134	.43	.211	.20	−.277	**.01**
MRICP vs. 4th Vent.	−.251	.13	.102	.55	−.325	**.005**
ICCI vs. HBV/PCFV	.030	.86	−.033	.84	−.219	.06
ICCI vs. PCFV/ICV	−.032	.85	.038	.82	.206	.08
ICCI vs. PCFV	.114	.51	−.207	.21	.156	.18
ICCI vs. 4th Vent.	.469	**.004**	−.218	.20	.261	**.02**
ICVC vs. HBV/PCFV	−.150	.38	.353	**.03**	−.115	.33
ICVC vs. PCFV/ICV	−.121	.48	−.026	.88	.095	.42
ICVC vs. PCFV	.334	**.04**	.252	.13	.359	**.002**
ICVC vs. 4th Vent.	.394	**.01**	−.188	.27	.221	.06

Neurosurgery. Author manuscript; available in PMC 2016 May 04.